HHS Public Access

Author manuscript

Chem Res Toxicol. Author manuscript; available in PMC 2024 November 13.

Published in final edited form as:

Chem Res Toxicol. 2021 April 19; 34(4): 1004–1015. doi:10.1021/acs.chemrestox.1c00012.

Investigation of 2′-Deoxyadenosine-derived Adducts Specifically Formed in Rat Liver and Lung DNA by *N*′-Nitrosonornicotine (NNN) Metabolism

Yupeng Li,
Erik S. Carlson[1],
Adam T. Zarth,
Pramod Upadhyaya,
Stephen S. Hecht*
Masonic Cancer Center, University of Minnesota, Minneapolis, Minnesota 55455, United States.

Abstract

The International Agency for Research on Cancer has classified the tobacco-specific nitrosamines *N*′-nitrosonornicotine (NNN) and 4-(methylnitrosamino)-1-(3-pyridyl)-1-butanone (NNK) as “carcinogenic to humans” (Group 1). To exert its carcinogenicity, NNN requires metabolic activation to form reactive intermediates which alkylate DNA. Previous studies have identified cytochrome P450s-catalyzed 2′-hydroxylation and 5′-hydroxylation of NNN as major metabolic pathways, with preferential activation through the 5′-hydroxylation pathway in some cultured human tissues and patas monkeys. So far, the only DNA adducts identified from NNN 5′-hydroxylation in rat tissues are 2-[2-(3-pyridyl)-*N*-pyrrolidinyl]-2′-deoxyinosine (Py-Py-dI), 6-[2-(3-pyridyl)-*N*-pyrrolidinyl]-2′-deoxynebularine (Py-Py-dN), and N^6-[4-hydroxy-1-(pyridine-3-yl)butyl]-2′-deoxyadenosine (N^6-HPB-dAdo) after reduction. To expand the DNA adduct panel formed by NNN 5′-hydroxylation and identify possible activation biomarkers of NNN metabolism, we investigated the formation of dAdo-derived adducts using a new highly sensitive and specific LC-NSI-HRMS/MS method. Two types of NNN-specific dAdo-derived adducts, N^6-[5-(3-pyridyl)tetrahydrofuran-2-yl]-2′-deoxyadenosine (N^6-Py-THF-dAdo) and 6-[2-(3-pyridyl)-*N*-pyrrolidinyl-5-hydroxy]-2′-deoxynebularine (Py-Py(OH)-dN), were observed for the first time in calf thymus DNA incubated with 5′-acetoxyNNN. More importantly, Py-Py(OH)-dN was also observed in relatively high abundance in the liver and lung DNA of rats treated with racemic NNN in the drinking water for 3 weeks. These new adducts were

*To whom correspondence should be addressed: Masonic Cancer Center, University of Minnesota, 2231 6th Street SE - 2-148 CCRB, Minneapolis, MN 55455, USA. fax: (612) 624-3869; hecht002@umn.edu.
[1]Current address: Department of Chemistry and Chemical Biology, Harvard University, 12 Oxford St., Cambridge, MA 02138, USA

The authors declare no competing financial interest.

ASSOCIATED CONTENT

Supporting Information

The Supporting Information is available free of charge on the ACS Publications website at www.acs.org:
Reaction details (Schemes S1-2) and NMR data of synthesized dAdo-derived adducts (Figures S1-2, S4-6); HPLC traces of Py-Py(OH)-dN (Figure S3); mass spectrometric analysis of synthesized dAdo-derived adducts (Figures S7-8); MS^2 and MS^3 fragmentation patterns of each peak of N^6-Py-THF-dAdo diastereomers (Figure S9); Py-Py-dN was readily observed in $NaBH_3CN$-reduced calf thymus DNA samples but not in $NaBH_4$-reduced samples (Figure S10); representative LC conditions for the analysis of N^6-Py-THF-dAdo and Py-Py-dN (Tables S1-2).

characterized using authentic synthesized standards. Both NMR and MS data agreed well with the proposed structures of N^6-Py-THF-dAdo and Py-Py(OH)-dN. Reduction of Py-Py(OH)-dN by $NaBH_3CN$ led to the formation of Py-Py-dN both *in vitro* and *in vivo*, which was confirmed by its isotopically labelled internal standard [pyridine-D_4]Py-Py-dN. The NNN-specific dAdo adducts Py-THF-dAdo and Py-Py(OH)-dN formed by NNN 5′-hydroxylation provide a more comprehensive understanding of the mechanism of DNA adduct formation by NNN.

Graphical Abstract

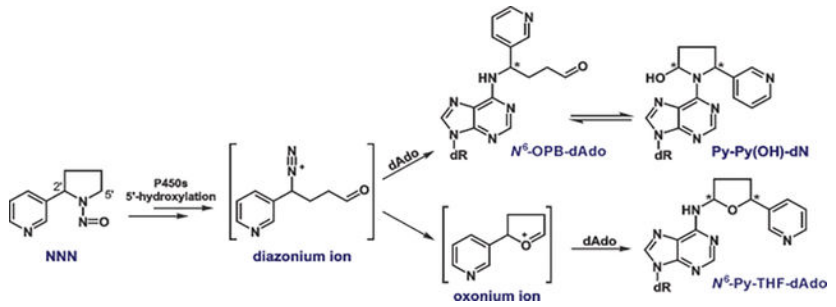

INTRODUCTION

Smokeless tobacco including chewing tobacco, snuff, snus, and related products comprise noncombustible tobacco products. While the tobacco industry promotes smokeless tobacco as less harmful than combustible tobacco, many of these products contain significant amounts of the tobacco-specific nitrosamine carcinogens *N*-nitrosonornicotine (NNN) and 4-(methylnitrosamino)-1-(3-pyridyl)-1-butanone (NNK) (Scheme 1). Levels ranged from 2.2 to 42.6 μg/g for NNN and 0.38 to 9.9 μg/g for NNK in the 40 top-selling brands of moist snuff – the most popular smokeless tobacco product – sold in the United States in 2004.[1] An updated survey in 2015 suggested a general decrease but still relatively high NNN levels in 34 smokeless tobacco products, ranging from 0.64 to 12.0 μg/g dry weight.[2] The U.S. FDA has proposed regulating levels of NNN in finished smokeless tobacco products at a maximum of 1 μg/g dry weight.[3,4] Current use of smokeless tobacco is still alarming. According to the 2019 National Youth Tobacco Survey, 3.5% of high school and middle school students, or a total of 940,000 students in the United States reported current use of smokeless tobacco products.[5]

Multiple epidemiological studies demonstrate that smokeless tobacco use increases the risk of precancerous lesions of the oral cavity[6,7] and leads to oral, pharyngeal and esophageal cancers.[6,8–10] NNN is considered the chemical carcinogen likely responsible for these types of cancer.[11,12] In a carcinogenicity study in rats, NNN caused esophageal cancer when administered at 5 ppm in the drinking water.[13] Similarly, chronic administration of racemic NNN (28 ppm) in the drinking water for 17 months to rats produced a high incidence of oral and esophageal cancer.[12] Nasal tumors predominated in rats treated with NNN by subcutaneous injection.[14–16] Tracheal and nasal tumors were also mainly observed in Syrian golden hamsters regardless of the administration pathways.[17–20] In a prospective nested case-control study carried out in Shanghai, cigarette smokers' urinary total NNN (free NNN

plus NNN-*N*-glucuronide) strongly predicted the future incidence of esophageal cancer.[21] Thus, NNN and the related carcinogen NNK, which always occur together in tobacco products, have been categorized as Group 1 carcinogens, “carcinogenic to humans” by the International Agency for Research on Cancer.[22]

Multiple studies have investigated mechanisms of carcinogenesis by tobacco-specific nitrosamines including NNN and NNK.[23–25] Cytochrome P450s-catalyzed metabolism is required to exert their carcinogenicity (Scheme 1).[23,26] For NNN, hydroxylation at the 5′- or 2′-position forms hydroxyNNNs **4** and **5**, respectively. They both spontaneously produce reactive intermediates (oxonium ion **8** and diazonium ion **9** from the 5′-hydroxylation pathway and diazonium ion **10** from the 2′-hydroxylation pathway), which are highly electrophilic and alkylate DNA to form different types of nucleobase adducts[27–33] and phosphate adducts.[34] Similarly, *α*-methyl and *α*-methylene hydroxylation metabolically activate NNK to form pyridyloxobutyl (POB) diazonium ion **10** and methyl diazonium ion **11**, respectively. They are both strongly electrophilic and form the corresponding POB and methyl DNA adducts.[35–42] NNK is also enzymatically reduced to its major metabolite 4-(methylnitrosamino)-1-(3-pyridyl)-1-butanol (NNAL), which also exerts strong carcinogenicity through a similar metabolic mechanism as described for NNK.[26]

Previous studies on the NNN 5′-hydroxylation pathway identified a panel of DNA adducts (Figure 1), mainly from the reaction of 2′-deoxynucleosides or calf thymus DNA with 5′-acetoxy-*N*′-nitrosonornicotine (5′-acetoxyNNN, **3**).[27,29] All the unreduced adducts **12**, **22** and **23** were only observed in the reaction mixture of 2′-deoxyadenosine (dAdo) or 2′-deoxyguanosine (dGuo) with **3**; the reduced adducts **19**, **24, 25** and **21**, **26** were observed in calf thymus DNA incubated with **3**. However, 2-[2-(3-pyridyl)-*N*-pyrrolidinyl]-2′-deoxyinosine (Py-Py-dI, **26**) was the only quantifiable adduct found in the tissues of rats treated with racemic NNN in the drinking water for 3 weeks. 6-[2-(3-Pyridyl)-*N*-pyrrolidinyl]-2′-deoxynebularine (Py-Py-dN, **21**) was barely observable in the lung and nasal mucosa from the same rats.[33] In the accompanying manuscript, we identified a new type of dAdo adduct N^6-[4-hydroxy-1-(pyridine-3-yl)butyl]-2′-deoxyadenosine (N^6-HPB-dAdo, **20**) *in vivo* after reduction, indicating the existence of its precursor adduct **13** before reduction.[43] This finding sparked our interest in performing a thorough investigation of all possible dAdo-derived adducts formed by NNN 5′-hydroxylation.

In the study presented here, we found that adducts N^6-[5-(3-pyridyl)tetrahydrofuran-2-yl]-2′-deoxyadenosine (N^6-Py-THF-dAdo, **12**, Scheme 1) and 6-[2-(3-pyridyl)-*N*-pyrrolidinyl-5-hydroxy]-2′-deoxynebularine (Py-Py(OH)-dN, **14**) were both formed in calf thymus DNA incubated with **3**. These two new adducts were structurally confirmed and characterized using authentic chemical standards. Importantly, adduct **14** was also observed in the liver and lung DNA of rats treated with NNN in the drinking water for 3 weeks. The formation of its reduced form Py-Py-dN (**21**) was also confirmed upon $NaBH_3CN$ reduction using the authentic chemical standard. The dAdo-derived adducts **12** and **14** specifically formed by NNN 5′-hydroxylation provide new insights pertinent to our understanding of mechanisms of carcinogenesis by NNN.

MATERIALS AND METHODS

Caution:

NNN and 5′-acetoxyNNN are strong carcinogens. They should be handled in a well-ventilated fume hood with extreme caution and with appropriate protective equipment.

Chemicals and supplies:

5′-AcetoxyNNN was obtained from our accompanying study.[43] Chemical standards of N^6-Py-THF-dAdo and Py-Py-dN were synthesized using the method described before.[29] Their corresponding isotopically labeled internal standards [$^{13}C_{10}{}^{15}N_5$]N^6-Py-THF-dAdo and [pyridine-D_4]Py-Py-dN were synthesized as described below, as was Py-Py(OH)-dN. [$^{15}N_5$]Py-Py-dI was obtained from our previous study.[33] 6-Chloropurine-2′-deoxyriboside (CAS number 4594–45-0) was purchased from Alfa Aesar (Tewksbury, MA). (*R,S*)-Nornicotine and [pyridine-D_4](*R,S*)-nornicotine and [$^{13}C_{10}{}^{15}N_5$]2′-deoxyadenosine were procured from Toronto Research Chemicals Inc. (Toronto, Ontario, Canada). Purified DNA hydrolysis enzymes and porcine liver esterase were from our accompanying study.[43] All other chemicals and supplies were purchased from Sigma-Aldrich or Fisher Scientific. Milli-Q H_2O was routinely used unless otherwise mentioned.

N^6-[5-(3-Pyridyl)tetrahydrofuran-2-yl]-2′-deoxyadenosine (12, N^6-Py-THF-dAdo):

N^6-Py-THF-dAdo was synthesized using the method described before.[29] The synthetic scheme is shown in supplementary Scheme S1. NMR data agreed with most of the reported values except for a few revisions including peak assignments of adenine-N^6-NH, THF-H_5 and THF-H_{4b} (Figure S1). High-resolution MS (HRMS) also confirmed the structure. The newly synthesized N^6-Py-THF-dAdo was essentially identical to our previous standard[29] but was quantified by quantitative ^{1}H NMR.[44] ^{1}H NMR (500 MHz, DMSO-d_6) δ 8.56 (d, J = 2.2 Hz, 1H, pyr-H_2), 8.48 (dd, J = 4.8, 1.7 Hz, 1H, pyr-H_6), 8.44 (d, J = 1.5 Hz, 1H, ade-H_8), 8.29 (s, 1H, ade-H_2), 7.77 (dt, J = 7.9, 2.1 Hz, 1H, pyr-H_4), 7.37 (dd, J = 7.9, 4.7 Hz, 1H, pyr-H_5), 6.48 (brs, 1H, -NH), 6.38 (t, J = 6.9 Hz, 1H, 1′-H), 5.32 (d, J = 4.0 Hz, 1H, 3′-OH), 5.16 (q, J = 5.6, 4.9 Hz, 1H, 5′-OH), 5.12 – 5.05 (m, 1H, THF-H_2), 5.06 – 4.92 (m, 1H, THF-H_5), 4.53 – 4.36 (m, 1H, 3′-H), 3.88 (t, J = 3.7 Hz, 1H, 4′-H), 3.63 (dd, J = 11.1, 5.2 Hz, 1H, 5′-H_a), 3.53 (q, J = 6.7, 5.8 Hz, 1H, 5′-H_b), 2.72 (ddd, J = 13.3, 7.8, 5.7 Hz, 1H, 2′-H_a), 2.54 (d, J = 1.5 Hz, 1H, THF-H_{3a}), 2.42 – 2.34 (m, 1H, THF-H_{4a}), 2.28 (ddd, J = 9.2, 6.5, 3.5 Hz, 1H, 2′-H_b), 2.19 – 1.94 (m, 1H, THF-H_{4b}), 1.78 (dq, J = 12.1, 8.6 Hz, 1H, THF-H_{3b}). HRMS (Orbitrap Fusion): $[M+H]^+$ calc'd 399.1775; found 399.1775.

[$^{13}C_{10}{}^{15}N_5$]N^6-[5-(3-Pyridyl)tetrahydrofuran-2-yl]-2′-deoxyadenosine ([$^{13}C_{10}{}^{15}N_5$]N^6-Py-THF-dAdo):

[$^{13}C_{10}{}^{15}N_5$]N^6-Py-THF-dAdo was synthesized analogously to N^6-Py-THF-dAdo. Its structure was confirmed by NMR and HRMS. Reaction details and ^{1}H NMR spectrum can be found in Scheme S1 and Figure S2, respectively. The product was obtained as a colorless oil (0.29 mg, 0.9%). ^{1}H NMR (500 MHz, DMSO-d_6) δ 8.65 (d, J = 11.4 Hz, 1H, pyr-H_2), 8.56 (d, J = 2.2 Hz, 1H, pyr-H_6), 8.51 – 8.41 (m, 1H, ade-H_8), 8.30 – 7.98 (m, 1H, ade-H_2), 7.77 (dt, J = 8.1, 2.0 Hz, 1H, pyr-H_4), 7.37 (dd, J = 7.9, 4.8 Hz, 1H, pyr-H_5), 6.37 (d, 0.5 H,

0.5 H, 1′-H), 5.09 (dd, J = 8.5, 6.2 Hz, 1H, THF-H_2), 5.06 – 4.91 (m, 1H, THF-H_5), 4.41 (d, 0.5 H, 0.5 H, 1′-H), 4.05 – 3.69 (m, 1H, 4′-H), 3.69 (dd, J = 28.7, 9.6 Hz, 1H, 5′-H_a), 3.50 – 3.36 (m, 1H, 5′-H_b), 2.85 (s, 1H, 2′-H_a), 2.50 (overlapped, 1H, THF-H_{3a})2.45 – 2.41 (m, 1H, THF-H_{4a}), 2.39 – 2.19 (m, 1H, 2′-H_b), 2.19 – 1.93 (m, 1H, THF-H_{4b}), 1.78 (dq, J = 12.3, 8.2, 7.7 Hz, 1H, THF-H_{3b}). HRMS (Orbitrap Fusion): $[M+H]^+$ calc'd 414.1963; found 414.1962.

6-[2-(3-Pyridyl)-*N*-pyrrolidinyl-5-hydroxy]-2′-deoxynebularine (14, Py-Py(OH)-dN):

Py-Py(OH)-dN was synthesized as illustrated in Scheme 2, starting with the newly identified dAdo adduct N^6-HPB-dAdo (**20**).[43] To a solution of **20** (0.03 mmol, 12 mg) in DMSO (0.5 mL) were added Dess-Martin periodinane (0.033 mmol, 14 mg) and Et_3N (0.15 mmol, 21 μL). The mixture was stirred at room temperature for 24 h. After reaction, the mixture was subjected directly to reverse phase HPLC purification as described in our accompanying study.[43] The desired product was collected at retention time 27.4 min. However, it was converted to 4 peaks after evaporation of the solvents (MeOH and H_2O) (Figure S3A). This mixture was separated into 3 fractions (7.1 min, 8.5 min, 14.9 min) under isocratic conditions (50% MeOH in H_2O, 15 min running time for each injection), the first two of which were collected and evaporated. Re-injections of the fractions collected for the peaks at 7.1 min and 8.5 min using the same LC method showed the separation of the same 4 peaks (Figure S3B). This strongly indicated that the synthesized compound Py-Py(OH)-dN contained multiple isomers likely including 4 diastereomers of Py-Py(OH)-dN (**14**) and its equilibrated ring open form N^6-OPB-dAdo (**13**) which consisted of 2 diastereomers. The desired product Py-Py(OH)-dN was collected as a colorless oil (0.57 mg, 5%). NMR spectra of Py-Py(OH)-dN are shown in Figure S4. ^{1}H NMR (500 MHz, DMSO-d_6) δ 8.62 (1H, pyr-H_2), 8.43 – 8.34 (1H, pyr-H_6), 8.28 (1H, ade-H_8), 8.12 (1H, ade-H_2), 7.75 (1H, pyr-H_4), 7.29 (1H, pyr-H_5), 6.51 – 6.33 (m, 1H, 1′-H), 6.23 (1H, pyrrolidine-C$\underline{H}$(OH)-), 5.51 (s, 1H, pyrrolidine-C$\underline{H}$-pyr), 5.31 (s, 1H, 3′-OH), 5.09 (s, 1H, 5′-OH), 4.41 (s, 1H, 3′-H), 3.87 (s, 1H, 4′-H), 3.60 (s, 1H, 5′-H_a), 3.48 (s, 1H, 5′-H_b), 2.80 – 2.60 (m, 1H, 2′-H_a), 2.45 (s, 1H, pyrrolidine-C$\underline{H}_{2a}$CH-pyr), 2.33 – 2.19 (m, 1H, 2′-H_b), 2.11 (s, 1H, pyrrolidine-C$\underline{H}_{2a}$CH(OH)-), 2.02 – 1.89 (m, 2H, pyrrolidine-C$\underline{H}_{2b}$CH-pyr and pyrrolidine-C$\underline{H}_{2b}$CH(OH)-). HRMS (Orbitrap Fusion): $[M+H]^+$ calc'd 399.1775; found 399.1778.

6-[2-(3-Pyridyl)-*N*-pyrrolidinyl]-2′-deoxynebularine (21, Py-Py-dN).

Py-Py-dN was synthesized as described.[29] The reaction details and NMR data are presented in Scheme S2 and Figure S5. The desired compound was obtained as a colorless oil (11 mg, 73%) and quantified by quantitative ^{1}H NMR.[44] ^{1}H NMR (500 MHz, DMSO-d_6) δ 8.45 (s, 1H, pyr-H_2), 8.38 (s, 1H, pyr-H_6), 8.38 (s, 0.5H, ade-H_8), 8.29 (s, 0.5H, ade-H_2), 8.19 (s, 0.5H, ade-$H_{8'}$), 8.05 (s, 0.5H, ade-$H_{2'}$), 7.55 (d, J = 7.3 Hz, 1H, pyr-H_4), 7.27 (dd, J = 7.5, 5.0 Hz, 1H, pyr-H_5), 6.33 (s, 1H, 1′-H), 6.20 (s, 0.5H, pyrrolidine-C$\underline{H}_a$-pyr), 5.52 (s, 0.5H, pyrrolidine-C$\underline{H}_b$-pyr), 5.28 (s, 1H, 3′-OH), 5.13 (s, 1H, 5′-OH), 4.42 (s, 0.5H, pyrrolidine-C$\underline{H}_{2a}$(N)-), 4.38 (s, 1H, 3′-H), 4.23 (s, 0.5H, pyrrolidine-C$\underline{H}_{2a'}$(N)-), 4.11– 4.01 (m, 0.5H, pyrrolidine-C$\underline{H}_{2b}$(N)-), 3.85 (s, 1H, 4′-H), 3.79 (s, 0.5H, pyrrolidine-C$\underline{H}_{2b'}$(N)-), 3.58 (s, 1H, 5′-H_a), 3.50 (s, 1H, 5′-H_b), 2.67 (s, 1H, 2′-H_a), 2.42 (s, 1H, pyrrolidine-C$\underline{H}_{2a}$CH-pyr), 2.24 (s, 1H, 2′-H_b), 2.11 – 1.82 (m, 3H, pyrrolidine-C$\underline{H}_{2b}$CH-pyr and pyrrolidine-C$\underline{H}_2$CH_2(N)-). ^{13}C NMR (126 MHz, DMSO-d_6) δ 152.4 (ade-C_6), 152.0

(ade-C_2), 149.3 (ade-C_4), 147.6 (pyr-C_2), 147.5 (pyr-C_6), 139.1 (overlapped, ade-C_8 and pyr-C_3), 133.2 (pyr-C_4), 123.3 (pyr-C_5), 119.9 (ade-C_5), 87.9 ($C_{4'}$), 83.7 ($C_{1'}$), 70.9 (doublet peak, $C_{3'}$), 61.8 ($C_{5'}$), 61.8 (pyrrolidine-CH(N)-), 59.4 (pyrrolidine-CH-pyr), 39.8 ($C_{2'}$), 34.9 (pyrrolidine-CH_2CH-pyr), 23.7 (pyrrolidine-CH_2CH_2(N)-). HRMS (Orbitrap Fusion): $[M+H]^+$ calc'd 383.1826; found 383.1828.

[Pyridine-D_4]6-[2-(3-pyridyl)-*N*-pyrrolidinyl]-2′-deoxynebularine (21, [pyridine-D_4]Py-Py-dN).

[Pyridine-D_4]Py-Py-dN was synthesized in the same way as Py-Py-dN (Scheme S2), and was obtained as a colorless oil (11 mg, 95%). NMR spectra are available in Figure S6. ^{1}H NMR (500 MHz, DMSO-d_6) δ 8.38 (s, 0.5H, ade-H_8), 8.29 (s, 0.5H, ade-H_2), 8.18 (s, 0.5H, ade-$H_{8'}$), 8.05 (s, 0.5H, ade-$H_{2'}$), 6.33 (s, 1H, 1′-H), 6.20 (s, 0.5H, pyrrolidine-CH_a-pyr), 5.52 (s, 0.5H, pyrrolidine-CH_b-pyr), 5.28 (s, 1H, 3′-OH), 5.13 (s, 1H, 5′-OH), 4.42 (s, 0.5H, pyrrolidine-CH_{2a}(N)-), 4.38 (s, 1H, 3′-H), 4.23 (s, 0.5H, pyrrolidine-$CH_{2a'}$(N)-), 4.04 (s, 0.5H, pyrrolidine-CH_{2b}(N)-), 3.85 (s, 1H, 4′-H), 3.77 (s, 0.5H, pyrrolidine-$CH_{2b'}$(N)-), 3.58 (s, 1H, 5′-H_a), 3.50 (s, 1H, 5′-H_b), 2.67 (s, 1H, 2′-H_a), 2.42 (s, 1H, pyrrolidine-CH_{2a}CH-pyr), 2.24 (s, 1H, 2′-H_b), 2.08 – 1.80 (m, 3H, pyrrolidine-CH_{2b}CH-pyr and pyrrolidine-CH_2CH_2(N)-). ^{13}C NMR (126 MHz, DMSO-d_6) δ 152.4 (ade-C_6), 151.8 (ade-C_2), 149.8 (ade-C_4), 147.3 (overlapped, pyr-C_2 and pyr-C_6), 139.2 (overlapped, ade-C_8 and pyr-C_3), 132.8 (pyr-C_4), 123.3 (pyr-C_5), 119.6 (ade-C_5), 87.9 ($C_{4'}$), 83.7 ($C_{1'}$), 70.9 (doublet peak, $C_{3'}$), 61.8 ($C_{5'}$), 61.8 (pyrrolidine-CH(N)-), 59.2 (pyrrolidine-CH-pyr), 39.8 ($C_{2'}$), 33.6 (pyrrolidine-CH_2CH-pyr), 23.4 (pyrrolidine-CH_2CH_2(N)-). HRMS (Orbitrap Fusion): $[M+H]^+$ calc'd 387.2077; found 387.2078.

DNA sample preparation without reduction:

Calf thymus DNA incubated with 5′-acetoxyNNN and liver and lung DNA of rats treated with racemic NNN in their drinking water for 3 weeks were obtained from our previous studies.[33,43] They were prepared similarly as described before except for not adding the reducing reagent $NaBH_3CN$ or $NaBH_4$. The internal standard [$^{13}C_{10}{}^{15}N_5$]N^6-Py-THF-dAdo (10 fmol) was added prior to enzyme hydrolysis. To prepare the spiked samples for the analysis of Py-Py(OH)-dN, calf thymus DNA or rat DNA was analyzed by MS prior to adding synthesized Py-Py(OH)-dN. The spiked samples were then re-analyzed under the same conditions.

DNA sample preparation with reduction:

DNA samples were prepared essentially as described in our accompanying study.[43] Briefly, when using $NaBH_3CN$ as the reducing agent, to the isolated DNA (~50 μg) dissolved in 500 μL of 10 mM sodium succinate buffer containing 5 mM $CaCl_2$ was added 100 μL 20 mg/mL $NaBH_3CN$ in the succinate buffer. The mixture was incubated at 37 °C for 1 h. Then the internal standards [pyridine-D_4]Py-Py-dN (10 fmol) and [$^{15}N_5$]Py-Py-dI (10 fmol) [pyridine-D_4]Py-Py-dN were added, followed by 3 purified hydrolytic enzymes deoxyribonuclease I (0.4 units), phosphodiesterase I (0.1 units), and alkaline phosphatase (0.8 units). The mixture was allowed to incubate at 37 °C overnight for a complete DNA hydrolysis. The hydrolysate was filtered with 10K filters (Microcon-10 filter, Millipore) at 14,000 *g* for 1 h at 4 °C. When using $NaBH_4$ as the reducing agent, 100 μL 20 mg/mL $NaBH_4$ in the succinate buffer was added to the DNA hydrolysate and incubated for 1 h.

The resulting mixture was adjusted to pH ~8.0 by adding ~50 μL 1 N HCl solution. The hydrolysate was similarly filtered as described above. A small fraction of the hydrolysate (10 μL) was taken for dGuo quantitation by HPLC.[43] The remaining hydrolysate was purified with 33 mg Strata-X cartridges and the analyte was finally dissolved in 10 μL H_2O (Fisher, Optima®) prior to the MS analysis.

Mass spectrometric analysis of dAdo-derived adducts:

DNA hydrolysates were similarly analyzed by the liquid chromatography-nano-electrospray ionization-high-resolution tandem mass spectrometry (LC-NSI-HRMS/MS) method described in our accompanying study.[43] Table S1 describes the LC conditions that successfully resolved the newly identified dAdo-derived adducts, and in particular the 4 diastereomers of N^6-Py-THF-dAdo. New LC conditions to form sharp peaks of Py-Py(OH)-dN and to allow simultaneous detection of Py-Py-dN and Py-Py-dI are described in Table S2. Parameters of the high-resolution mass spectrometer with Orbitrap detector (Thermo Scientific™ Orbitrap Fusion™ Tribrid™) were basically the same except for using the masses of precursor ions of targeted analytes in this study. Precursor ions and MS^2 and MS^3 product ions characteristic of each analyte are summarized in Table 1. Proposed fragmentation patterns corresponding to Table 1 data can be found in Figures S7 and S8.

RESULTS

Our accompanying study characterized a structurally unique dAdo adduct N^6-HPB-dAdo (**20**, Scheme 1) *in vitro* and *in vivo* after reduction.[43] This adduct was hypothesized to result from the reduction of its precursor N^6-[4-oxo-1-(pyridine-3-yl)butyl]-2′-deoxyadenosine (N^6-OPB-dAdo, **13**). In addition, a putative adduct N^6-Py-THF-dAdo (**12**) was initially observed when investigating new DNA phosphate adducts formed by NNN 5′-hydroxylation (unpublished data). Collectively, those results encouraged us to perform a detailed study of dAdo-derived adducts formed by NNN 5′-hydroxylation.

Synthesis and characterization of chemical standards

N^6-Py-THF-dAdo (**12**) and [$^{13}C_{10}{}^{15}N_5$]N^6-Py-THF-dAdo were readily synthesized using the method reported before.[29] Both one- and two-dimensional NMR data confirmed their structures (Figures S1 and S2). HRMS analysis suggested that the most abundant MS^2 product ions were *m/z* 283.1302 and 293.1321 for N^6-Py-THF-dAdo and [$^{13}C_{10}{}^{15}N_5$]N^6-Py-THF-dAdo, respectively (Figure S7). They were both formed by the neutral loss of 2′-deoxyribose. Product ions from MS^3 transitions were also similar for both compounds, with the most abundant ions of *m/z* 148.0757 $[M+H\text{-dAdo}]^+$ and 136.0618 $[Ade+H]^+$ for N^6-Py-THF-dAdo, and 148.0757 $[M+H\text{-dAdo}]^+$ and 146.0637 $[[^{13}C_{10}{}^{15}N_5]Ade+H]^+$ for [$^{13}C_{10}{}^{15}N_5$]N^6-Py-THF-dAdo (Table 1). Chromatographic baseline resolution of the 4 diastereomers of each compound was successfully achieved under the LC conditions described in Table S1 (as shown in Figure 3 and Figure 5). Absolute configuration of the stereochemistry of each peak had been assigned previously,[29] however, was not pursued in this study.

Py-Py(OH)-dN (**14**) is the cyclic equilibrated form of N^6-OPB-dAdo (**13**) (Scheme 1). They were together hypothesized as products of NNN 5′-hydroxylation based on characterization of N^6-HPB-dAdo (**20**) after reduction.[43] Py-Py(OH)-dN was synthesized as illustrated in Scheme 2. Oxidation of N^6-HPB-dAdo (**20**) using Dess-Martin periodinane yielded N^6-OPB-dAdo, which spontaneously cyclized to Py-Py(OH)-dN during solvent evaporation. As shown in Figure S3, HPLC purification afforded a mixture of at least 4 peaks, which likely contained both the 4 diastereomers of Py-Py(OH)-dN and its equilibrated ring open form N^6-OPB-dAdo with 2 diastereomers. The ^{1}H NMR spectrum showed typical proton resonances consistent with the pyridine ring and nucleobase moiety of Py-Py(OH)-dN (Figure S4). However, absolute quantitation was not achieved due to the difficulty of accurately integrating each spectral peak for quantitative ^{1}H NMR analysis.

HRMS data agreed well with the proposed fragmentation pattern of Py-Py(OH)-dN (Figure 2). Interestingly, we noted that an ion of *m/z* 265.1197 $[M+H\text{-}dR\text{-}H_2O]^+$ was the second most predominant ion in the MS^2 transitions of Py-Py(OH)-dN. This ion was not observed in the MS^2 spectra of N^6-Py-THF-dAdo (Figure S7). Fragmentation of the most abundant ion *m/z* 283.1302 $[M+H\text{-}dR]^+$ led to the formation of *m/z* 136.0618 $[Ade+H]^+$ and *m/z* 148.0757 $[M+H\text{-}dAdo]^+$, both of which were also observed in the MS^3 transitions of N^6-Py-THF-dAdo. However, fragmentation of the unique ion *m/z* 265.1196 formed a product ion *m/z* 130.0651 $[M+H\text{-}dAdo\text{-}H_2O]^+$, which appeared to be characteristic of Py-Py(OH)-dN. Thus, transitions of *m/z* 399.2 → *m/z* 265.1196 and *m/z* 265.2 → *m/z* 130.0651 were chosen for the characterization of Py-Py(OH)-dN, distinguishing it from the nearly co-eluting peak of N^6-Py-THF-dAdo in the DNA samples (Figure 3).

Py-Py-dN (**21**), the reduced form of Py-Py(OH)-dN, and its isotopically labeled internal standard [pyridine-D_4]Py-Py-dN were synthesized as reported previously.[29] NMR data were consistent with reported values (Figures S5 and S6). Analysis by HRMS showed good agreement with the proposed fragmentation patterns (Figure S8). The predominant MS^2 transition of Py-Py-dN was *m/z* 383.2 $[M+H]^+$ → 267.1353 $[M+H\text{-}dR]^+$; the predominant MS^2 transition of [pyridine-D_4]Py-Py-dN was the corresponding *m/z* 387.2 to *m/z* 271.1604. It is noteworthy that MS^3 fragmentation of each compound required higher collision energy than usual. With an HCD collision energy setting at 75%, there were still substantial amounts of precursor ions unfragmented with both compounds (data not shown).

Detection of N^6-Py-THF-dAdo and Py-Py(OH)-dN *in vitro* without reduction

A highly sensitive and specific LC-NSI-HRMS/MS method was used for the analysis of dAdo-derived adducts without reduction. Analysis of hydrolysates of calf thymus DNA incubated with 5′-acetoxyNNN clearly showed the formation of N^6-Py-THF-dAdo (Figure 3). Four diastereomers of this adduct were resolved nicely, each of which co-eluted with the corresponding isomer of the internal standard [$^{13}C_{10}{}^{15}N_5$]N^6-Py-THF-dAdo. The representative MS^2 fragmentation pattern of N^6-Py-THF-dAdo agreed well with expectations. Both MS^2 and MS^3 fragmentation patterns of each of the 4 major peaks were essentially identical (Figure S9), further indicating the formation of N^6-Py-THF-dAdo containing 4 diastereomers in calf thymus DNA incubated with 5′-acetoxyNNN.

However, as depicted in Figure 3, there was a broad peak nearly co-eluting with N^6-Py-THF-dAdo. Mass spectrometric differences were clearly observed between this broad peak and N^6-Py-THF-dAdo. The presence of the precursor ion *m/z* 399.1771 and the formation of the unique product ions *m/z* 265.1195 and *m/z* 130.0650 suggested that this broad peak was Py-Py(OH)-dN. The extracted ion chromatogram of MS^2 transition *m/z* 399.2 → 265.1196 distinguished this peak nicely from N^6-Py-THF-dAdo (middle MS trace of Figure 3). An additional experiment with synthesized Py-Py(OH)-dN spiked into the calf thymus DNA showed the same but augmented peak area of Py-Py(OH)-dN (Figure 4). This strongly implied that Py-Py(OH)-dN was formed as the broad peak *in vitro* as shown in Figure 3. It is noteworthy that Py-Py(OH)-dN peak shown in Figure 4 is relatively sharper than in Figure 3 when new LC conditions were applied as described in Table S2. However, this new method could not resolve the peaks of N^6-Py-THF-dAdo from the massive peak of Py-Py(OH)-dN (Figure 5B).

Detection of Py-Py(OH)-dN but not N^6-Py-THF-dAdo *in vivo* without reduction

Similarly, the hydrolysates of liver and lung DNA of rats treated with 500 ppm racemic NNN in the drinking water for 3 weeks were analyzed by the LC-NSI-HRMS/MS method. As shown in Figure 4, clear peaks of Py-Py(OH)-dN, determined by its characteristic MS^2 transition of *m/z* 399.2 → 265.1196 and MS^3 transition of *m/z* 265.1 → 130.0651, were observed in the rat liver and lung DNA. A similar spiking experiment as described above also confirmed the formation of Py-Py(OH)-dN in the rat tissues. No such Py-Py(OH)-dN peak was observed in the liver and lung DNA of control rats from the same study given tap water only.

However, it was interesting that no such N^6-Py-THF-dAdo peaks were observed in any *in vivo* DNA samples used for this study. As shown in Figure 5A, [$^{13}C_{10}{}^{15}N_5$]N^6-Py-THF-dAdo was at least partially resolved from the massive peak of Py-Py(OH)-dN. No peaks co-eluted with the isomers of [$^{13}C_{10}{}^{15}N_5$]N^6-Py-THF-dAdo in the rat lung DNA, which suggested the absence of N^6-Py-THF-dAdo. Considering that N^6-Py-THF-dAdo was readily formed *in vitro* (Figure 3), this could indicate a high efficiency of repair towards this type of DNA damage *in vivo*, at least in the liver and lung tissues of rats examined in this study.

Detection of Py-Py-dN *in vitro* and *in vivo* upon reduction

Py-Py(OH)-dN has been detected in relatively high MS abundance both *in vitro* and *in vivo*, as shown in Figures 4 and 5. However, it was difficult to accurately quantify due to its broad peak shape ($W_{baseline}$ = ~10 min) and the complexity of the synthesized standard. Based on our experience with Py-Py-dI quantitation,[33] it seemed reasonable to reduce Py-Py(OH)-dN to Py-Py-dN for quantitation. However, Py-Py(OH)-dN was not fully reduced using 2 mg $NaBH_3CN$ as in our previous studies of Py-Py-dI.[29,33] Increased amounts of $NaBH_3CN$ (up to 10 mg) improved the conversion rate but significantly affected the enzymatic hydrolysis of DNA. Instead, 2 mg $NaBH_4$ nearly completely converted Py-Py(OH)-dN to its reduced form Py-Py-dN when added into the hydrolysate after enzymatic hydrolysis (data not shown).

Surprisingly, Py-Py-dN, the reduced form of Py-Py(OH)-dN which has been readily observed both *in vitro* and *in vivo*, was barely detected in the same DNA samples reduced by $NaBH_4$. However, it was clearly observed in $NaBH_3CN$-reduced samples (Figure 6 and Figure S10). The formation of the two diastereomers of Py-Py-dI in the same DNA samples suggested that this unexpected result was not due to experimental errors with the reduction procedure. The equilibrium between Py-Py(OH)-dN and N^6-OPB-dAdo (Scheme 1) is hypothesized to be responsible for the missing detection of Py-Py-dN in samples treated with $NaBH_4$. This will be discussed further in the Discussion section.

DISCUSSION

In this study, we characterized two types of NNN-specific DNA adducts - N^6-Py-THF-dAdo (**12**, Scheme 1) and Py-Py(OH)-dN (**14**). Both are formed in calf thymus DNA treated with 5′-acetoxyNNN and, more importantly, Py-Py(OH)-dN was for the first time observed in the DNA of rats treated with racemic NNN. The structure and presence of both adducts were confirmed by the authentic chemical standards. Py-Py-dN, the reduced form of Py-Py(OH)-dN, was also detected in rat DNA samples reduced by $NaBH_3CN$. The two new adducts characterized here, together with N^6-HPB-dAdo (**20**), characterized in the companion study[43], provide a more comprehensive understanding of the mechanism of DNA damage by NNN.

N^6-Py-THF-dAdo was previously characterized in the reaction mixture of dAdo with 5′-acetoxyNNN;[29] however, it was not observed in treated calf thymus DNA until now. An important aspect of the current study is the use of HRMS, which provides significantly improved sensitivity and specificity to distinguish the peaks of targeted analytes from background noise. The observed peaks of N^6-Py-THF-dAdo in our calf thymus DNA sample were unique, with 4 baseline-resolved peaks, each of which showed essentially identical MS^2 and MS^3 product ion patterns (Figures S9). This strongly indicated that those peaks represented 4 isomers of one single compound. The MS^2 product ion *m/z* 283.1302 (formed by neutral loss of 2′-deoxyribose) and its corresponding MS^3 product ion *m/z* 136.0617 $[Ade+H]^+$ suggested that this compound contained 2′-dAdo. Thus, a possible dAdo-derived adduct N^6-Py-THF-dAdo which contains 2 chiral centers with an exact mass of *m/z* 399.1775 was proposed to be the observed adduct in the treated calf thymus DNA sample. Using the authentic synthesized standards, those peaks were confirmed unambiguously as the 4 diastereomers of N^6-Py-THF-dAdo. However, no such peaks were observed from any *in vivo* DNA samples. This may imply that N^6-Py-THF-dAdo, if formed in rat DNA, is efficiently repaired by a mechanism yet to be studied.

The tetrahydrofuranyl dAdo adducts formed by NNN were undetectable in rat liver and lung DNA in this study. This was similar to the results we obtained in hepatic DNA of rats treated with *N*-nitrosopyrrolidine (NPYR). As a strong rat hepatocarcinogen and a model compound for the study of NNN, NPYR has been found to form tetrahydrofuranyl (THF) adducts with all 4 nucleobases *in vitro* and *in vivo*.[45–48] However, the overall levels of all those THF-type base adducts (quantified after reduction) were significantly lower than other adducts formed by NPYR.[49] The dAdo-derived adduct N^6-(4-hydroxybut-1-yl)-2′-deoxyadenosine (N^6-(4-HOB)dAdo) was in particularly low abundance compared to the other nucleobase-derived

adducts, occurred at levels of 0.02 – 0.04 μmol/mol dGuo (or 20 – 40 fmol/μmol dGuo) in the liver DNA of rats treated with 200 or 600 ppm NPYR in the drinking water for various times.[48] Albeit the low levels of N^6-(4-HOB)dAdo in rat liver DNA, it might be of greater biological importance than other analogous adducts to cause the predominant AT to GC transition in the mutants of NPYR-treated Sprague–Dawley gpt δ transgenic rats.[50]

Initial characterization of Py-Py(OH)-dN was difficult due to its very similar chromatographic behavior to N^6-Py-THF-dAdo. After extensive optimization of the LC conditions, a very shallow linear gradient as depicted in Table S1 successfully resolved the Py-Py(OH)-dN peak from the 4 diastereomers of N^6-Py-THF-dAdo (Figure 3). Unique features of *m/z* 265.1196 in MS^2 transitions and *m/z* 130.0618 in MS^3 transitions were found to be characteristic to Py-Py(OH)-dN. This was likely due to the hemiaminal moiety of Py-Py(OH)-dN that could lose a molecule of H_2O during fragmentation (Figure 2).

For the quantitation of Py-Py(OH)-dN in rat liver and lung DNA samples, the reducing strategy used for the Py-Py-dI study was adopted here. However, reported conditions using $NaBH_3CN$ did not achieve a complete reduction of Py-Py(OH)-dN.[28, 32] The optimized reducing condition of adding $NaBH_4$ into the DNA hydrolysate after enzymatic hydrolysis led to a nearly quantitative conversion. It is noteworthy that reducing agents can interfere with enzymatic hydrolysis under the conditions described before.[28,32] $NaBH_4$ strongly inhibited the hydrolysis process (with pH adjusted) at the amount of 2 mg if added prior to the enzymatic hydrolysis step. Extra washing steps by filtering undigested DNA with H_2O or succinate buffer did not solve the problem.[51] On the contrary, $NaBH_3CN$ was well tolerated by the hydrolytic enzymes at the amount of 2 mg but started showing inhibitory effect at higher amounts. The underlying mechanism is unclear but seems to be related with the boronate ions formed by the solvolysis of these two reducing agents.

The formation of Py-Py-dN (**21**, Scheme 1) in calf thymus DNA incubated with 5′-acetoxyNNN and rat liver and lung DNA was expected upon $NaBH_3CN$ reduction, since its precursor Py-Py(OH)-dN was readily detected in those samples. However, it was surprisingly unexpected to barely detect this adduct in the same DNA samples upon $NaBH_4$ reduction as shown in Figure 6 and Figure S10. Considering that Py-Py(OH)-dN is in equilibrium with N^6-OPB-dAdo (Scheme 1) in the DNA hydrolysates, it seems possible that a stronger reducing agent such as $NaBH_4$ favors the reduction of N^6-OPB-dAdo versus Py-Py(OH)-dN, and thus leads to the predominant formation of N^6-HPB-dAdo. In contrast, $NaBH_3CN$ is likely to reduce both N^6-OPB-dAdo and the Schiff base **18** (hypothetically formed by Py-Py(OH)-dN) to a similar extent to form both of their corresponding reduced products N^6-HPB-dAdo (**20**) and Py-Py-dN (**21**). This is consistent with the results obtained in our accompanying study, in which levels of N^6-HPB-dAdo were generally lower in DNA samples reduced by $NaBH_3CN$ versus $NaBH_4$.[43] Considering that Py-Py-dI was formed in a similar mechanism,[33] its decreased levels in DNA samples reduced by $NaBH_4$ compared to those reduced by $NaBH_3CN$ as observed in Figure 6 and Figure S10 might also be the same cause.

One of the biomarkers used for monitoring tobacco carcinogen uptake in smokeless tobacco users is NNAL, a reliable biomarker specifically for NNK exposure which can also reflect

relevant uptake of other tobacco carcinogens.[52] However, this biomarker does not directly reflect the level of NNN, which is frequently present in relatively high quantities in smokeless tobacco products.[53] NNN is the most abundant tobacco-specific carcinogen in unburned tobacco.[1,2] One direct biomarker for NNN exposure which was applied in the Shanghai Cohort Study is urinary total NNN.[21] However, the level of urinary total NNN does not reflect the metabolic fate of NNN, and only accounted for less than 1% of dosed NNN in the patas monkey.[54] Thus, identification of new NNN-specific biomarkers such as NNN-specific DNA adducts that can reflect NNN uptake and metabolic activation is of high interest to us. As depicted in Scheme 1, NNN 2′-hydroxylation forms the same diazonium ion **10** as the *α*-methyl hydroxylation of NNK. The convergence of this alkylating intermediate makes the origin of resulting DNA adducts such as 7-(4-(3-pyridyl)-4-oxobut-1-yl)guanine (7-POB-Gua) or O^2-(4-(3-pyridyl)-4-oxobut-1-yl)thymidine (O^2-POB-Thd) indistinguishable from the two tobacco-specific nitrosamine carcinogens. However, NNN 5′-hydroxylation forms oxonium ion **8** and diazonium ion **9**, both of which are structurally unique. DNA adducts formed by alkylation of those two reactive intermediates are structurally specific to NNN metabolism. Besides, the 5′-hydroxylation pathway of NNN is more prevalent than 2′-hydroxylation in some cultured human tissues[15,55–59] and in the patas monkey.[54] Thus, products formed by NNN 5′-hydroxylation such as N^6-Py-THF-dAdo and Py-Py(OH)-dN characterized in this study have potential to be NNN-specific metabolic activation biomarkers in people who use tobacco products.

In summary, we have characterized the formation of two NNN-specific DNA adducts N^6-Py-THF-dAdo and Py-Py(OH)-dN in calf thymus DNA incubated with 5′-acetoxyNNN using authentic synthesized chemical standards. More importantly, Py-Py(OH)-dN was for the first time detected in the liver and lung DNA of rats treated with racemic NNN. Its reduced form Py-Py-dN was also confirmed in the same DNA samples reduced by $NaBH_3CN$. The results of this study provide a better understanding of the mechanism of carcinogenesis caused by the tobacco-specific carcinogen NNN.

Supplementary Material

Refer to Web version on PubMed Central for supplementary material.

ACKNOWLEDGMENTS

The authors thank Dr. Peter W. Villalta and Dr. Yingchun Zhao for help with the operation of the mass spectrometer. We also thank Bob Carlson for his editorial assistance. Yupeng would like to thank Dr. Bin Ma for his valuable suggestions with mass spectrometric analysis.

Funding

This study was supported by grant CA-81301 from the National Cancer Institute. Mass spectrometry was carried out in the Analytical Biochemistry Shared Resource of the Masonic Cancer Center, University of Minnesota, supported in part by Cancer Center Support Grant CA-077598.

ABBREVIATIONS

NNN	*N*′-nitrosonornicotine
NNK	4-(methylnitrosamino)-1-(3-pyridyl)-1-butanone

FDA	Food and Drug Administration
POB	pyridyloxobutryl
NNAL	4-(methylnitrosamino)-1-(3-pyridyl)-1-butanol
5′-acetoxyNNN	5′-acetoxy-*N*′-nitrosonornicotine
dAdo	2′-deoxyadenosine
dGuo	2′-deoxyguanosine
Py-Py-dI	2-[2-(3-pyridyl)-*N*-pyrrolidinyl]-2′-deoxyinosine
Py-Py-dN	6-[2-(3-pyridyl)-*N*-pyrrolidinyl]-2′-deoxynebularine
***N*^{6}-HPB-dAdo**	*N*^{6}-[4-hydroxy-1-(pyridine-3-yl)butyl]-2′-deoxyadenosine
***N*^{6}-Py-THF-dAdo**	*N*^{6}-[5-(3-pyridyl)tetrahydrofuran-2-yl]-2′-deoxyadenosine
Py-Py(OH)-dN	6-[2-(3-pyridyl)-*N*-pyrrolidinyl-5-hydroxy]-2′-deoxynebularine
$NaBH_3CN$	sodium cyanoborohydride
$NaBH_4$	sodium borohydride
***N*^{6}-PHB-dAdo**	*N*^{6}-[4-(3-pyridyl)-4-hydroxy-1-butyl]-2′-deoxyadenosine
MS	mass spectrometry
HRMS	high-resolution mass spectrometry
$NaBH_4$	sodium borohydride
LC-NSI-HRMS/MS	liquid chromatography-nano-electrospray ionization-high-resolution tandem mass spectrometry
SPE	solid phase extraction
HCD	higher-energy collisional dissociation
AGC	automatic gain control
LOD	limit of detection
LOQ	limit of quantitation
CV	coefficient of variation
NYPR	*N*-nitrosopyrrolidine
***N*^{6}-(4-HOB)dAdo**	*N*^{6}-(4-hydroxybut-1-yl)-2′-deoxyadenosine

REFERENCES

1. Richter P, Hodge K, Stanfill S, Zhang L, and Watson C (2008) Surveillance of moist snuff total nicotine, pH, moisture, un-ionized nicotine, and tobacco-specfic nitrsoamine content. Nicotine Tob Res 10, 1645–1652. [PubMed: 18988077]
2. Ammann JR, Lovejoy KS, Walters MJ, and Holman MR (2016) A survey of *N*′-nitrosonornicotine (NNN) and total water content in select smokeless tobacco products purchased in the United States in 2015. J Agric Food Chem 64, 4400–4406. [PubMed: 27192054]
3. U.S. Food and Drug Administration. (2017) Tobacco product standard for *N*-nitrosonornicotine level in finished smokeless tobacco products. Fed Regist 82, 8004–8053.
4. Berman ML, and Hatsukami DK (2018) Reducing tobacco-related harm: FDA's proposed product standard for smokeless tobacco. Tob Control 27, 352–354. [PubMed: 28634163]
5. Wang TW, Gentzke AS, Creamer MR, Cullen KA, Holder-Hayes E, Sawdey MD, Anic GM, Portnoy DB, Hu S, et al. (2019) Tobacco product use and associated factors among middle and high school students - United States, 2019. Mmwr Surveill Summ 68, 1–22.
6. Boffetta P, Hecht S, Gray N, Gupta P, and Straif K (2008) Smokeless tobacco and cancer. Lancet Oncol 9, 667–675. [PubMed: 18598931]
7. Khan Z, Khan S, Christianson L, Rehman S, Ekwunife O, and Samkange-Zeeb F (2017) Smokeless tobacco and oral potentially malignant disorders in South Asia: A systematic review and meta-analysis. Nicotine Tob Res 20, 12–21. [PubMed: 27928050]
8. Gupta B, and Johnson NW (2014) Systematic review and meta-analysis of association of smokeless tobacco and of betel quid without tobacco with incidence of oral cancer in South Asia and the Pacific. PLoS One 9, e113385. [PubMed: 25411778]
9. Khan Z, Tönnies J, and Müller S (2014) Smokeless tobacco and oral cancer in South Asia: a systematic review with meta-analysis. J Cancer Epidemiol 2014, 394696. [PubMed: 25097551]
10. Sinha DN, Abdulkader RS, and Gupta PC (2016) Smokeless tobacco-associated cancers: A systematic review and meta-analysis of Indian studies. Int J Cancer 138, 1368–1379. [PubMed: 26443187]
11. Stepanov I, Sebero E, Wang R, Gao YT, Hecht SS, and Yuan JM (2014) Tobacco-specific *N*-nitrosamine exposures and cancer risk in the Shanghai Cohort Study: remarkable coherence with rat tumor sites. Int J Cancer 134, 2278–2283. [PubMed: 24243522]
12. Balbo S, James-Yi S, Johnson CS, O'Sullivan MG, Stepanov I, Wang M, Bandyopadhyay D, Kassie F, Carmella S, et al. (2013) (S)-*N*′-Nitrosonornicotine, a constituent of smokeless tobacco, is a powerful oral cavity carcinogen in rats. Carcinogenesis 34, 2178–2183. [PubMed: 23671129]
13. Stoner GD, Adams C, Kresty LA, Hecht SS, Murphy SE, and Morse MA (1998) Inhibition of *N*′-nitrosonornicotine-induced esophageal tumorigenesis by 3-phenylpropyl isothiocyanate. Carcinogenesis 19, 2139–2143. [PubMed: 9886569]
14. Hecht SS, Chen CB, Ohmori T, and Hoffmann D (1980) Comparative carcinogenicity in F344 rats of the tobacco-specific nitrosamines, *N*′-nitrosonornicotine and 4-(*N*-methyl-*N*-nitrosamino)-1-(3-pyridyl)-1-butanone. Cancer Res 40, 298–302. [PubMed: 7356512]
15. Castonguay A, Rivenson A, Trushin N, Reinhardt J, Spathopoulos S, Weiss CJ, Reiss B, and Hecht SS (1984) Effects of chronic ethanol consumption on the metabolism and carcinogenicity of *N*′-nitrosonornicotine in F344 rats. Cancer Res 44, 2285–2290. [PubMed: 6722769]
16. Hoffmann D, Rivenson A, Amin S, and Hecht SS (1984) Dose-response study of the carcinogenicity of tobacco-specific *N*-nitrosamines in F344 rats. J Cancer Res Clin Oncol 108, 81–86. [PubMed: 6746721]
17. Hilfrich J, Hecht SS, and Hoffmann D (1977) A study of tobacco carcinogenesis. XV. Effects of *N*′-nitrosonornicotine and *N*′-nitrosoanabasine in Syrian golden hamsters. Cancer Lett 2, 169–175. [PubMed: 837363]
18. Hoffmann D, Castonguay A, Rivenson A, and Hecht SS (1981) Comparative carcinogenicity and metabolism of 4-(methylnitrosamino)-1-(3-pyridyl)-1-butanone and *N*′-nitrosonornicotine in Syrian golden hamsters. Cancer Res 41, 2386–2393. [PubMed: 7237437]

19. McCoy GD, Hecht SS, Katayama S, and Wynder EL (1981) Differential effect of chronic ethanol consumption on the carcinogenicity of *N*-nitrosopyrrolidine and *N*′-nitrosonornicotine in male Syrian golden hamsters. Cancer Res 41, 2849–2854. [PubMed: 7248945]
20. Hecht SS, Young R, and Maeura Y (1983) Comparative carcinogenicity in F344 rats and Syrian golden hamsters of *N*′-nitrosonornicotine and *N*′-nitrosonornicotine-1-*N*-oxide. Cancer Lett 20, 333–340. [PubMed: 6627230]
21. Yuan JM, Knezevich AD, Wang R, Gao YT, Hecht SS, and Stepanov I (2011) Urinary levels of the tobacco-specific carcinogen *N*′-nitrosonornicotine and its glucuronide are strongly associated with esophageal cancer risk in smokers. Carcinogenesis 32, 1366–1371. [PubMed: 21734256]
22. International Agency for Research on Cancer. (2007) Smokeless Tobacco and Some Tobacco-specific N-Nitrosamines, In IARC Monographs on the Evaluation of Carcinogenic Risks to Humans, v 89, IARC, Lyon, FR.
23. Hecht SS (1998) Biochemistry, biology, and carcinogenicity of tobacco-specific *N*-nitrosamines. Chem Res Toxicol 11, 559–603. [PubMed: 9625726]
24. Hecht SS (2003) Tobacco carcinogens, their biomarkers, and tobacco-induced cancer. Nature Rev Cancer 3, 733–744. [PubMed: 14570033]
25. Carlson ES, Upadhyaya P, and Hecht SS (2016) Evaluation of nitrosamide formation in the cytochrome P450-mediated metabolism of tobacco-specific nitrosamines. Chem Res Toxicol 29, 2194–2205. [PubMed: 27989137]
26. Jalas JR, Hecht SS, and Murphy SE (2005) Cytochrome P450 enzymes as catalysts of metabolism of 4-(methylnitrosamino)-1-(3-pyridyl)-1-butanone, a tobacco specific carcinogen. Chem Res Toxicol 18, 95–110. [PubMed: 15720112]
27. Upadhyaya P, McIntee EJ, Villalta PW, and Hecht SS (2006) Identification of adducts formed in the reaction of 5'-acetoxy-*N*′-nitrosonornicotine with deoxyguanosine and DNA. Chem Res Toxicol 19, 426–435. [PubMed: 16544948]
28. Lao Y, Yu N, Kassie F, Villalta PW, and Hecht SS (2007) Analysis of pyridyloxobutyl DNA adducts in F344 rats chronically treated with (*R*)- and (*S*)-*N*′-nitrosonornicotine. Chem Res Toxicol 20, 246–256. [PubMed: 17305408]
29. Upadhyaya P, and Hecht SS (2008) Identification of adducts formed in the reactions of 5'-acetoxy-*N*′-nitrosonornicotine with deoxyadenosine, thymidine, and DNA. Chem Res Toxicol 21, 2164–2171. [PubMed: 18821782]
30. Zhang S, Wang M, Villalta PW, Lindgren BR, Lao Y, and Hecht SS (2009) Quantitation of pyridyloxobutyl DNA adducts in nasal and oral mucosa of rats treated chronically with enantiomers of *N*′-nitrosonornicotine. Chem Res Toxicol 22, 949–956. [PubMed: 19405515]
31. Yang J, Villalta PW, Upadhyaya P, and Hecht SS (2016) Analysis of O^6-[4-(3-pyridyl)-4-oxobut-1-yl]-2'-deoxyguanosine and other DNA adducts in rats treated with enantiomeric or racemic *N*′-nitrosonornicotine. Chem Res Toxicol 29, 87–95. [PubMed: 26633576]
32. Zhao L, Balbo S, Wang M, Upadhyaya P, Khariwala SS, Villalta PW, and Hecht SS (2013) Quantitation of pyridyloxobutyl-DNA adducts in tissues of rats treated chronically with (*R*)- or (*S*)-*N*′-nitrosonornicotine (NNN) in a carcinogenicity study. Chem Res Toxicol 26, 1526–1535. [PubMed: 24001146]
33. Zarth AT, Upadhyaya P, Yang J, and Hecht SS (2016) DNA adduct formation from metabolic 5'-hydroxylation of the tobacco-specific carcinogen *N*′-nitrosonornicotine in human enzyme systems and in rats. Chem Res Toxicol 29, 380–389. [PubMed: 26808005]
34. Li Y, Ma B, Cao Q, Balbo S, Zhao L, Upadhyaya P, and Hecht SS (2019) Mass spectrometric quantitation of pyridyloxobutyl DNA phosphate adducts in rats chronically treated with *N*′-nitrosonornicotine. Chem Res Toxicol 32, 773–783. [PubMed: 30740971]
35. Balbo S, Johnson CS, Kovi RC, James-Yi SA, O'Sullivan MG, Wang M, Le CT, Khariwala SS, Upadhyaya P, et al. (2014) Carcinogenicity and DNA adduct formation of 4-(methylnitrosamino)-1-(3-pyridyl)-1-butanone and enantiomers of its metabolite 4-(methylnitrosamino)-1-(3-pyridyl)-1-butanol in F-344 rats. Carcinogenesis 35, 2798–2806. [PubMed: 25269804]
36. Ma B, Villalta PW, Zarth AT, Kotandeniya D, Upadhyaya P, Stepanov I, and Hecht SS (2015) Comprehensive high-resolution mass spectrometric analysis of DNA phosphate adducts formed by

the tobacco-specific lung carcinogen 4-(methylnitrosamino)-1-(3-pyridyl)-1-butanone. Chem Res Toxicol 28, 2151–2159. [PubMed: 26398225]

37. Leng J, and Wang Y (2017) Liquid chromatography-tandem mass spectrometry for the quantification of tobacco-specific nitrosamine-induced DNA adducts in mammalian cells. Anal Chem 89, 9124–9130. [PubMed: 28749651]
38. Ma B, Zarth AT, Carlson ES, Villalta PW, Stepanov I, and Hecht SS (2017) Pyridylhydroxybutyl and pyridyloxobutyl DNA phosphate adduct formation in rats treated chronically with enantiomers of the tobacco-specific nitrosamine metabolite 4-(methylnitrosamino)-1-(3-pyridyl)-1-butanol. Mutagenesis 32, 561–570. [PubMed: 29186507]
39. Carlson ES, Upadhyaya P, Villalta PW, Ma B, and Hecht SS (2018) Analysis and identification of 2'-deoxyadenosine-derived adducts in lung and liver DNA of F-344 rats treated with the tobacco-specific carcinogen 4-(methylnitrosamino)-1-(3-pyridyl)-1-butanone and enantiomers of its metabolite 4-(methylnitrosamino)-1-(3-pyridyl)-1-butanol. Chem Res Toxicol 31, 358–370. [PubMed: 29651838]
40. Ma B, Zarth AT, Carlson ES, Villalta PW, Upadhyaya P, Stepanov I, and Hecht SS (2018) Identification of more than 100 structurally unique DNA-phosphate adducts formed during rat lung carcinogenesis by the tobacco-specific nitrosamine 4-(methylnitrosamino)-1-(3-pyridyl)-1-butanone. Carcinogenesis 39, 232–241. [PubMed: 29194532]
41. Guo S, Leng J, Tan Y, Price NE, and Wang Y (2019) Quantification of DNA lesions induced by 4-(methylnitrosamino)-1-(3-pyridyl)-1-butanol in mammalian cells. Chem Res Toxicol 32, 708–717. [PubMed: 30714728]
42. Ma B, Villalta PW, Hochalter JB, Stepanov I, and Hecht SS (2019) Methyl DNA phosphate adduct formation in lung tumor tissue and adjacent normal tissue of lung cancer patients. Carcinogenesis 40, 1387–1394. [PubMed: 30873516]
43. Li Y, and Hecht SS Identification of an *N*'-nitrosonornicotine-specific deoxyadenosine adduct in rat liver and lung DNA. Chem Res Toxicol submitted.
44. Pauli GF, Chen SN, Simmler C, Lankin DC, Godecke T, Jaki BU, Friesen JB, McAlpine JB, and Napolitano JG (2014) Importance of purity evaluation and the potential of quantitative (1)H NMR as a purity assay. J Med Chem 57, 9220–9231. [PubMed: 25295852]
45. Wang M, Young-Sciame R, Chung FL, and Hecht SS (1995) Formation of N^2-tetrahydrofuranyl and N^2-tetrahydropyranyl adducts in the reactions of α-acetoxy-*N*-nitrosopyrrolidine and α-acetoxy-*N*-nitrosopiperidine with DNA. Chem Res Toxicol 8, 617–624. [PubMed: 7548743]
46. Young-Sciame R, Wang M, Chung FL, and Hecht SS (1995) Reactions of α-acetoxy-*N*-nitrosopyrrolidine and α-acetoxy-*N*-nitrosopiperidine with deoxyguanosine: formation of N^2-tetrahydrofuranyl and N^2-tetrahydropyranyl adducts. Chem Res Toxicol 8, 607–616. [PubMed: 7548742]
47. Wang M, Lao Y, Cheng G, Shi Y, Villalta PW, and Hecht SS (2007) Identification of adducts formed in the reaction of alpha-acetoxy-*N*-nitrosopyrrolidine with deoxyribonucleosides and DNA. Chem Res Toxicol 20, 625–633. [PubMed: 17394360]
48. Wang M, Lao Y, Cheng G, Shi Y, Villalta PW, Nishikawa A, and Hecht SS (2007) Analysis of adducts in hepatic DNA of rats treated with *N*-nitrosopyrrolidine. Chem Res Toxicol 20, 634–640. [PubMed: 17394361]
49. Loureiro AP, Zhang W, Kassie F, Zhang S, Villalta PW, Wang M, and Hecht SS (2009) Mass spectrometric analysis of a cyclic 7,8-butanoguanine adduct of *N*-nitrosopyrrolidine: comparison to other *N*-nitrosopyrrolidine adducts in rat hepatic DNA. Chem Res Toxicol 22, 1728–1735. [PubMed: 19761253]
50. Kanki K, Nishikawa A, Masumura K, Umemura T, Imazawa T, Kitamura Y, Nohmi T, and Hirose M (2005) *In vivo* mutational analysis of liver DNA in *gpt* delta transgenic rats treated with the hepatocarcinogens *N*-nitrosopyrrolidine, 2-amino-3-methylimidazo[4,5-*f*]quinoline, and di(2-ethylhexyl)phthalate. Mol Carcinog 42, 9–17. [PubMed: 15486947]
51. Carra A, Guidolin V, Dator RP, Upadhyaya P, Kassie F, Villalta PW, and Balbo S (2019) Targeted high resolution LC/MS^3 adductomics method for the characterization of endogenous DNA damage. Front Chem 7, 658. [PubMed: 31709223]

52. Stepanov I, and Hatsukami DK (2020) Chemical characterization of smokeless tobacco products and relevant exposures in users, In Smokeless Tobacco Products (Pickworth WB, Ed.) pp 121–150, Elsevier.

53. Edwards SH, Rossiter LM, Taylor KM, Holman MR, Zhang L, Ding YS, and Watson CH (2017) Tobacco-specific nitrosamines in the tobacco and mainstream smoke of U.S. commercial cigarettes. Chem Res Toxicol 30, 540–551. [PubMed: 28001416]

54. Upadhyaya P, Zimmerman CL, and Hecht SS (2002) Metabolism and pharmacokinetics of *N*′-nitrosonornicotine in the patas monkey. Drug Metab Dispos 30, 1115–1122. [PubMed: 12228188]

55. Hecht SS, Chen CH, McCoy GD, Hoffmann D, and Domellöf L (1979) Alpha-hydroxylation of *N*-nitrosopyrrolidine and *N*′-nitrosonornicotine by human liver microsomes. Cancer Lett 8, 35–41. [PubMed: 509417]

56. Castonguay A, Stoner GD, Schut HA, and Hecht SS (1983) Metabolism of tobacco-specific *N*-nitrosamines by cultured human tissues. Proc Natl Acad Sci 80, 6694–6697. [PubMed: 6579555]

57. Chakradeo PP, Nair J, and Bhide SV (1995) Metabolism of *N*′-nitrosonornicotine by adult and fetal human oesophagal cultures. Cell Biol Int 19, 53–58. [PubMed: 7613511]

58. Patten CJ, Smith TJ, Friesen MJ, Tynes RE, Yang CS, and Murphy SE (1997) Evidence for cytochrome P450 2A6 and 3A4 as major catalysts for *N*′-nitrosonornicotine alpha-hydroxylation by human liver microsomes. Carcinogenesis 18, 1623–1630. [PubMed: 9276639]

59. Jalas JR, Ding X, and Murphy SE (2003) Comparative metabolism of the tobacco-specific nitrosamines 4-(methylnitrosamino)-1-(3-pyridyl)-1-butanone and 4-(methylnitrosamino)-1-(3-pyridyl)-1-butanol by rat cytochrome P450 2A3 and human cytochrome P450 2A13. Drug Metab Dispos 31, 1199–1202. [PubMed: 12975327]

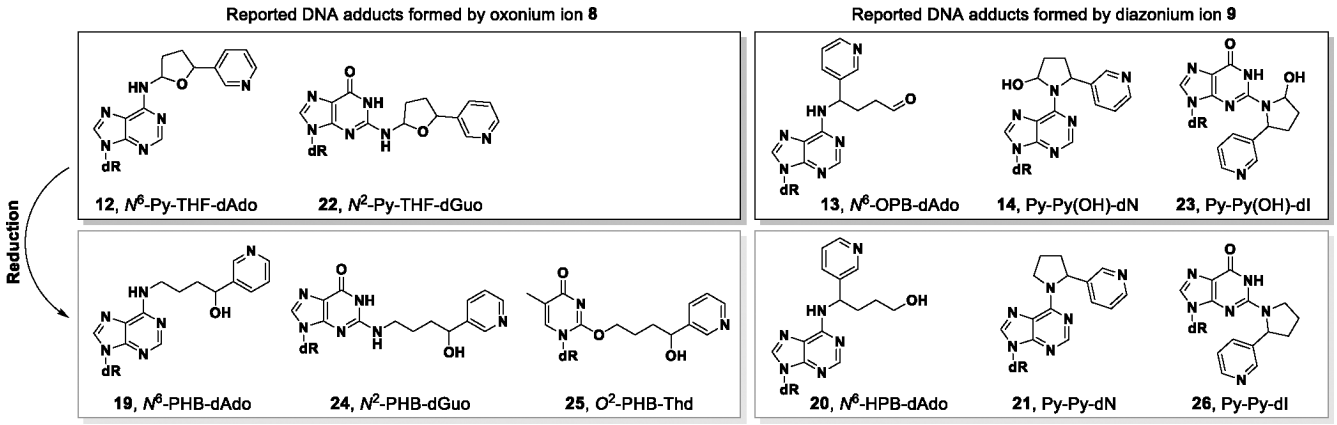

Figure 1.

Summary of DNA adducts formed by NNN 5′-hydroxylation *in vitro* and *in vivo*. dR = 2′-deoxyribose. Structures of oxonium ion **8** and diazonium ion **9** are shown in Scheme 1.

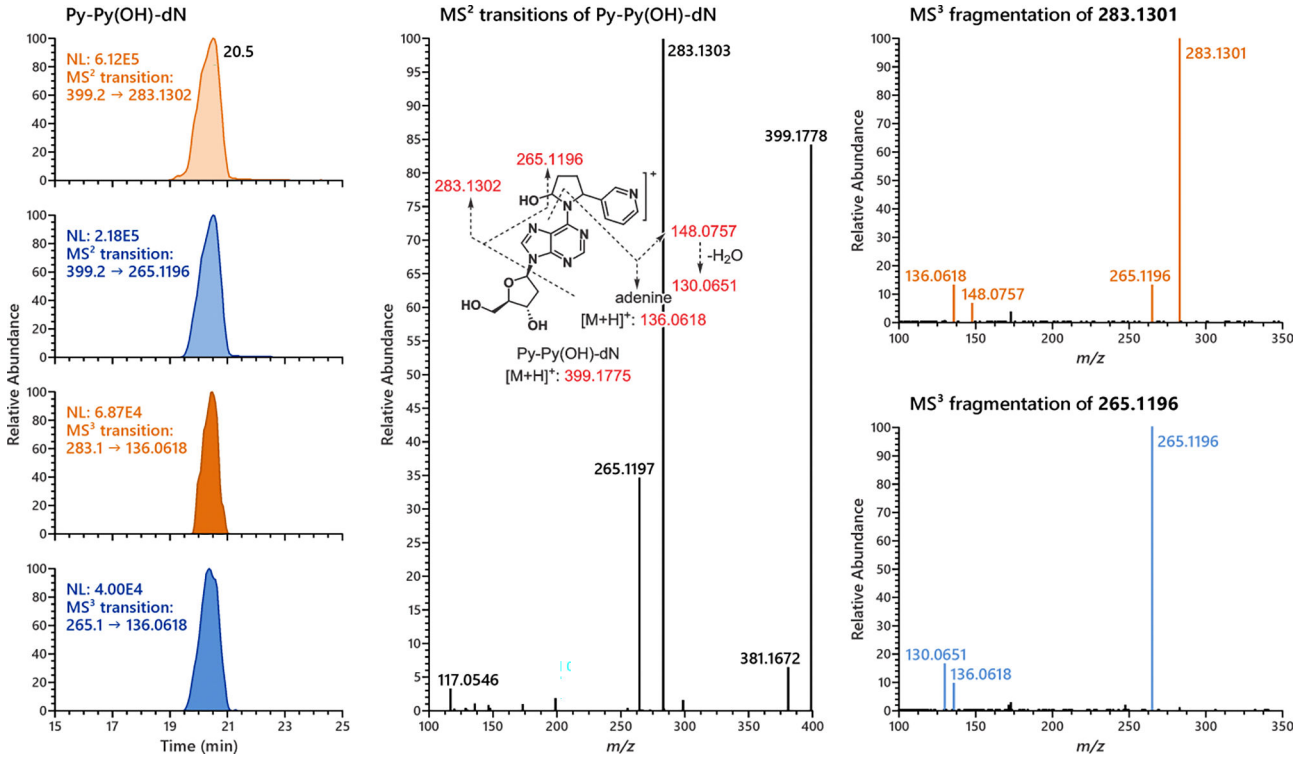

Figure 2.

Representative chromatograms and MS^2 and MS^3 product ion spectra of Py-Py(OH)-dN. The fragmentation patterns of MS^2 and MS^3 transitions of Py-Py(OH)-dN agreed well with proposed patterns.

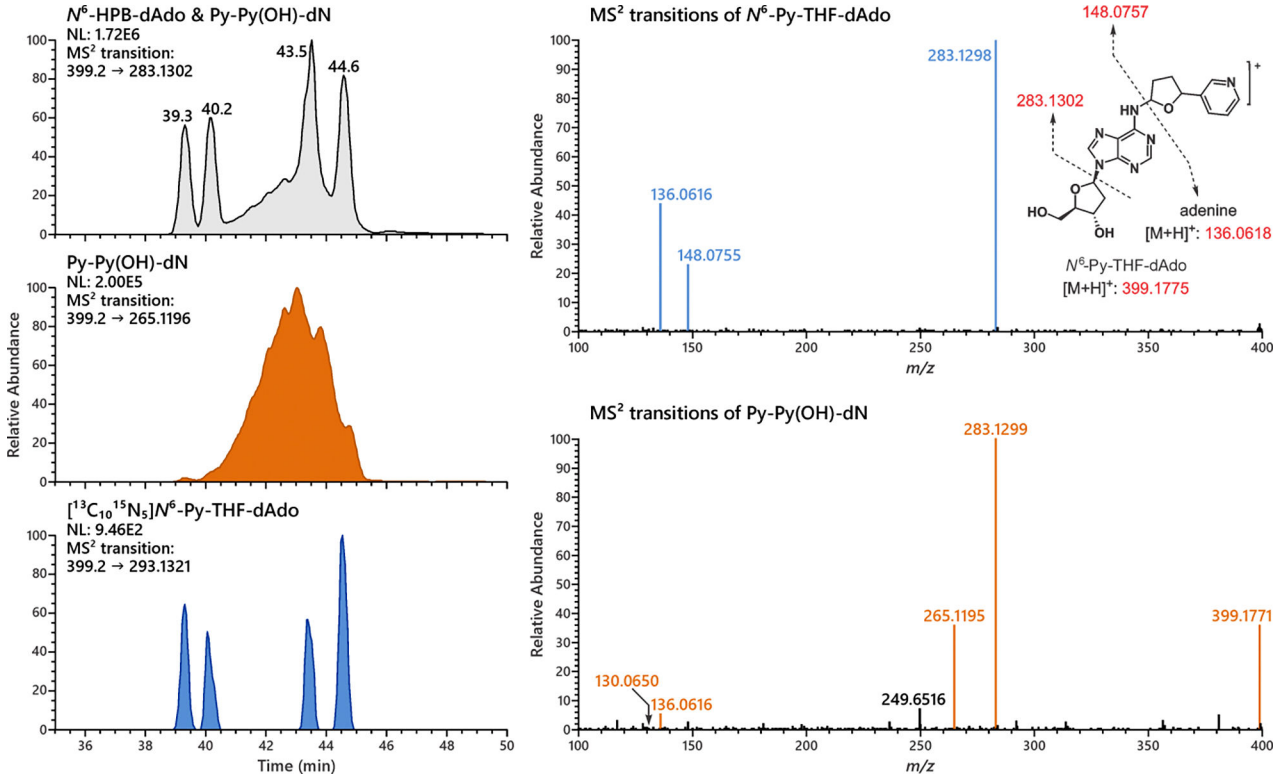

Figure 3.

Representative extracted product ion chromatograms of MS^2 transitions for the analysis of N^6-Py-THF-dAdo and Py-Py(OH)-dN formation in calf thymus DNA incubated with 5′-acetoxyNNN. Four diastereomer peaks of N^6-Py-THF-dAdo were observed from the MS^2 transition of 399.2 → 283.1302, co-eluting with the synthesized internal standard [$^{13}C_{10}{}^{15}N_5$]N^6-Py-THF-dAdo. However, a broad peak nearly co-eluting with N^6-Py-THF-dAdo was observed. It can form a unique MS^2 fragment ion 265.1195, which suggests its structure to be Py-Py(OH)-dN (see Figure 2 for the structure and fragmentation pattern of Py-Py(OH)-dN).

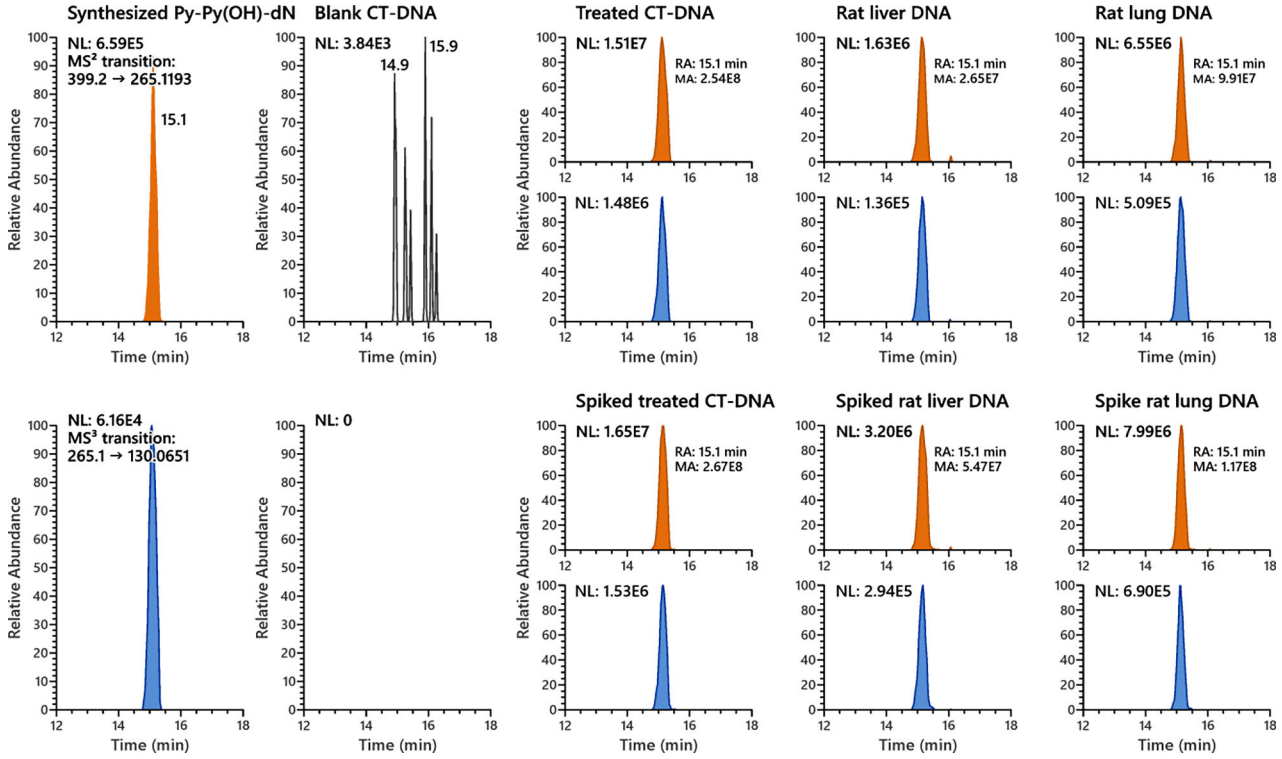

Figure 4.

Py-Py(OH)-dN was formed in calf thymus DNA incubated with 5′-acetoxyNNN and in the liver and lung DNA of rats treated with 500 ppm racemic NNN in the drinking water for 3 weeks. Synthesized Py-Py(OH)-dN spiked into the DNA samples co-eluted with the observed peak. No such Py-Py(OH)-dN peak was observed in an untreated control calf thymus DNA sample.

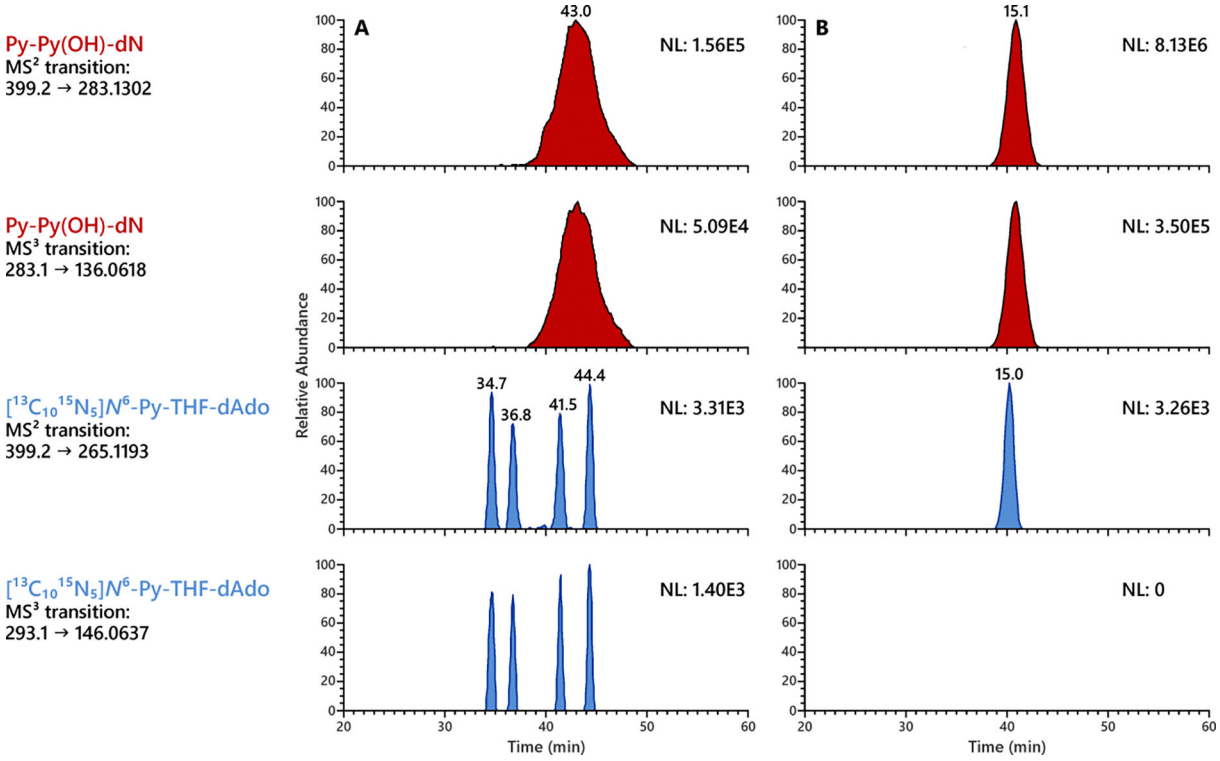

Figure 5.

Py-Py(OH)-dN (in red) but not N^6-Py-THF-dAdo (in blue) was observed in the lung DNA of rats treated with 500 ppm racemic NNN for 3 weeks. LC conditions are critical for resolving N^6-Py-THF-dAdo peaks from the massive peak of Py-Py(OH)-dN. (A) LC conditions depicted in Table S1 can separate the 4 diastereomers of N^6-Py-THF-dAdo and partially resolve it from Py-Py(OH)-dN, however causing a significantly broad peak of Py-Py(OH)-dN. (B) LC conditions depicted in Table S2 afford a sharper peak of Py-Py(OH)-dN but fail to resolve N^6-Py-THF-dAdo.

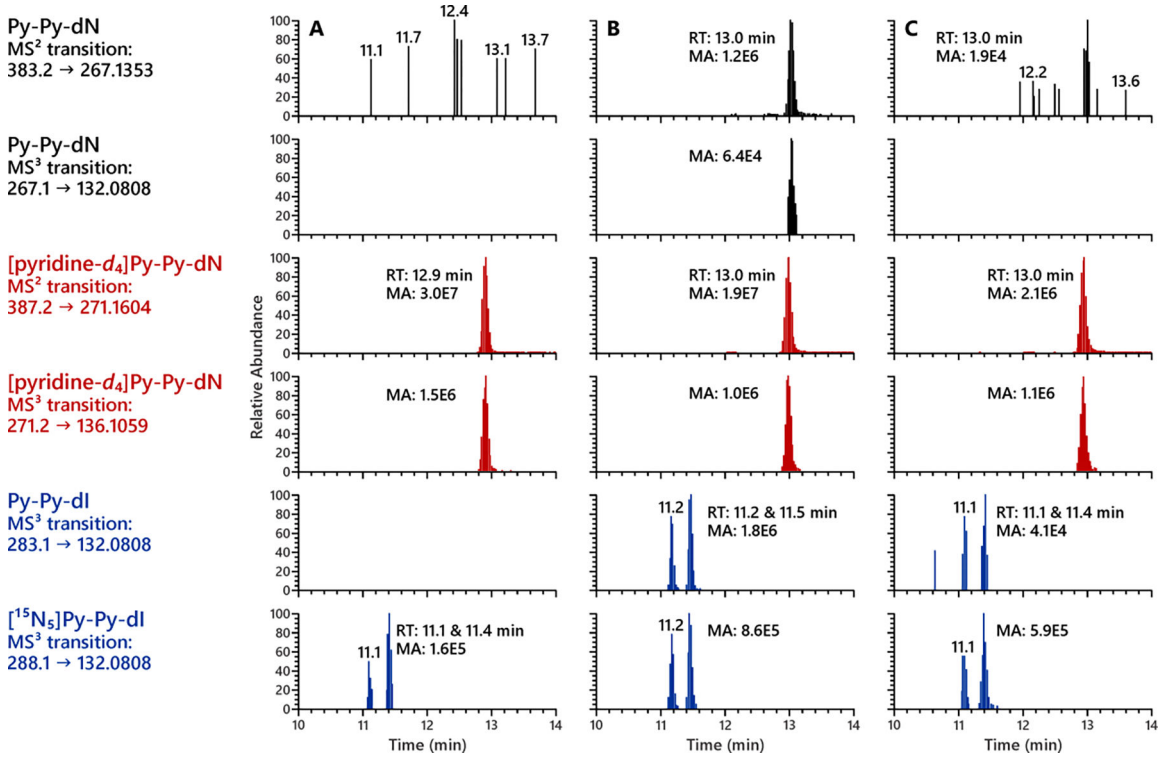

Figure 6.

Py-Py-dN was clearly observed in the lung DNA of rats reduced by $NaBH_3CN$ but not $NaBH_4$. (A) Untreated calf thymus DNA reduced with 2 mg $NaBH_3CN$; (B) lung DNA of rats treated with 500 ppm NNN reduced with 2 mg $NaBH_3CN$; (C) lung DNA of rats treated with 500 ppm NNN reduced with 2 mg $NaBH_4$.

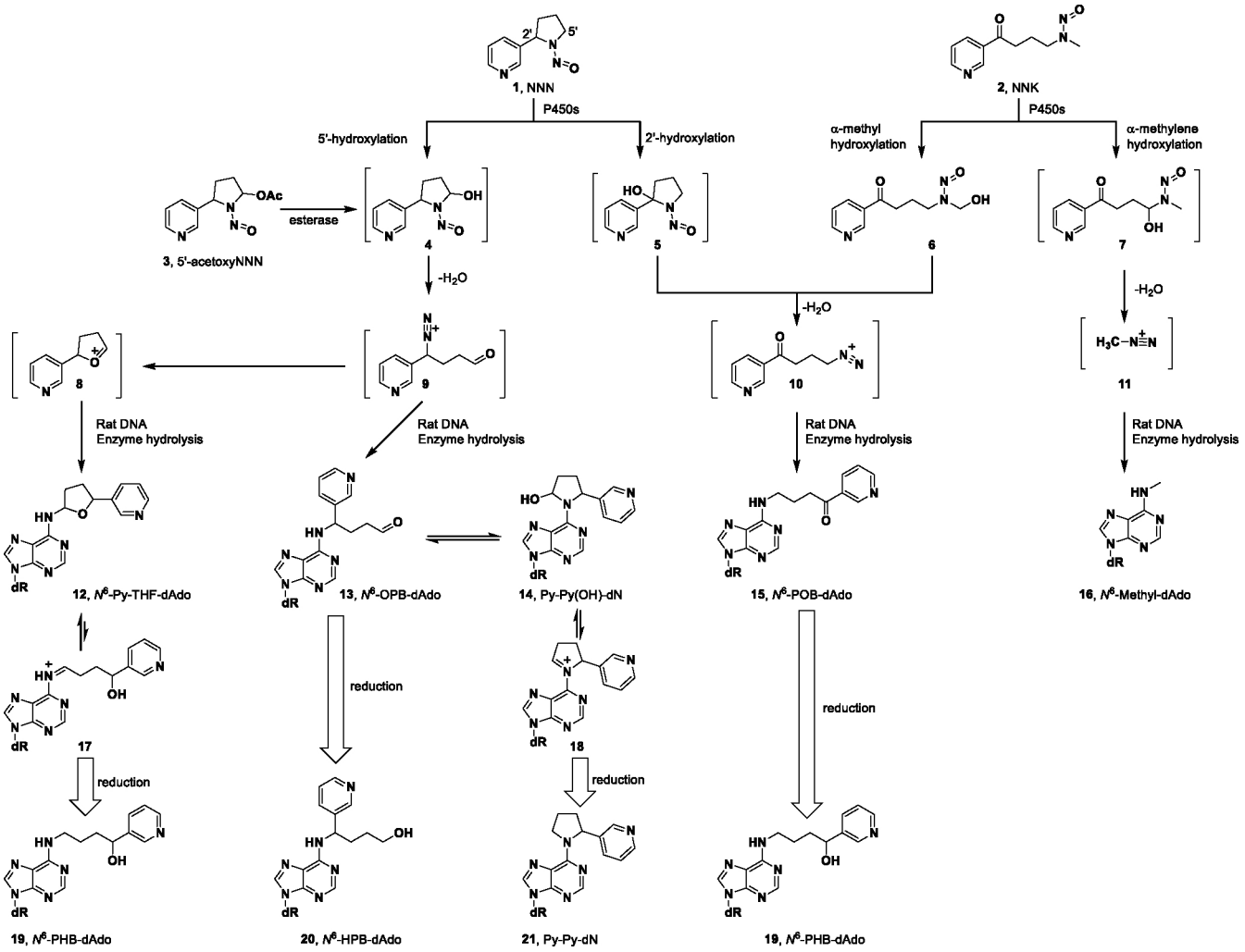

Scheme 1.

Mechanisms of dAdo-derived adduct formation from NNN and NNK metabolic activation catalyzed by cytochrome P450 enzymes.

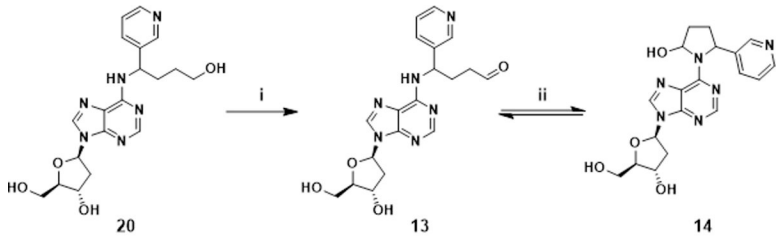

Reagents and Conditions: (i) Dess-Martin periodinane, Et_3N, DMSO, rt, 24 h; (ii) MeOH.

Scheme 2.

Synthetic route for Py-Py(OH)-dN (**14**).

Table 1.

Precursor ions and MS^2 and MS^3 product ions of dAdo-derived adducts.

	Fragment ions	N^6-Py-THF-dAdo	$[^{13}C_{10}{}^{15}N_5]N^6$-Py-THF-dAdo	Py-Py(OH)-dN	Py-Py-dN	[pyridine-D_4]Py-Py-dN
Precursor ion	$[M+H]^+$	399.1775	414.1963	399.1775	383.1826	387.2077
MS^2product ions	$[M+H-dR]^+$	283.1302	293.1321	283.1302	267.1353	271.1604
	$[M+H-dR-H_2O]^+$	ND	ND	265.1196	ND	ND
MS^3product ions	$[M+H-dAdo]^+$	148.0757	148.0757	148.0757	132.0808	136.1059
	$[M+H-dAdo-H_2O]^+$	ND	ND	130.0651	ND	ND
	$[Ade+H]^+$	136.0618	146.0637	136.0618	136.0618	136.0618

ND: not detected; dR: 2'-deoxyribose